MSI Journal of
Multidisciplinary Research (MSIJMR)

Volume: 3, Issue: 7 (July-2026)
Published by *MSI Publishers*
ISSN 3049-0669 (Online)

Received: 25-06-2026
Accepted: 03-07-2026
Published: 09-07-2026

Mathematical Analysis and Numerical Simulation of Magnetized Williamson Nanofluid Flow over a Rotating Stretching Surface with Joule Heating and Thermal Radiation

Authors Details

Omariba Geofrey Ong'era[1*]
Department of Pure and Applied Mathematics, Jomo Kenyatta University of Agriculture and Technology (JKUAT), Juja, Kenya.

Augustine Ayanga Mayaka[2]
Department of Pure and Applied Mathematics, Jomo Kenyatta University of Agriculture and Technology (JKUAT), Juja, Kenya.

ABSTRACT: This study investigates the flow behaviour of a magnetohydrodynamic (MHD) Williamson nanofluid over a rotating stretching surface, considering the combined effects of Joule heating and nonlinear thermal radiation. A mathematical model is developed to describe the transport phenomena by coupling the momentum, energy, and nanoparticle concentration equations under the influence of an applied magnetic field. The governing partial differential equations are rendered dimensionless and transformed into a system of nonlinear ordinary differential equations using appropriate similarity transformations. The resulting equations are solved numerically using the collocation method, and the computed results are validated through comparison with MATLAB bvp4c, demonstrating excellent agreement with percentage errors below 1%, which confirms the accuracy and reliability of the numerical approach. The effects of the magnetic parameter, Williamson parameter, Joule heating parameter, thermal radiation parameter, Brownian motion, thermophoresis, and rotational parameter on the velocity, temperature, and nanoparticle concentration profiles are presented graphically and discussed. The

 DOI: ***10.5281/zenodo.21276714***

engineering quantities of practical interest, namely the skin-friction coefficient, Nusselt number, and Sherwood number, are also evaluated. The results reveal that the magnetic field suppresses fluid velocity due to the Lorentz force, whereas Joule heating and thermal radiation significantly enhance the temperature distribution within the boundary layer. Brownian motion and thermophoresis increase nanoparticle diffusion and modify the concentration field, while the rotational effect enhances fluid motion near the stretching surface. The findings of this study provide useful insights into the design and optimization of thermal systems involving electrically conducting non-Newtonian nanofluids in engineering and industrial applications.

Keywords: *Magnetohydrodynamics, Williamson nanofluid, rotating stretching surface, Joule heating, thermal radiation, Brownian motion, thermophoresis, collocation method*

1. Background Information

Non-Newtonian fluids have attracted considerable attention due to their extensive applications in polymer processing, petroleum engineering, biomedical engineering, food industries, and chemical manufacturing. Unlike Newtonian fluids, whose viscosity remains constant regardless of the applied shear rate, non-Newtonian fluids exhibit viscosity that varies with the rate of deformation [1]. Among the various non-Newtonian fluid models, the Williamson fluid model has received significant attention because it accurately describes pseudoplastic (shear-thinning) fluids such as polymer melts, blood, paints, emulsions, and lubricants. Owing to its capability of representing the rheological behaviour of many industrial fluids, the Williamson model has become an important subject of mathematical and computational fluid dynamics research [2,3].

The interaction between electrically conducting fluids and externally applied magnetic fields is studied under magnetohydrodynamics (MHD). Magnetohydrodynamic flow has numerous engineering applications, including electromagnetic casting, crystal growth, liquid-metal cooling, plasma confinement, nuclear reactor cooling, MHD generators, and metallurgical processing [4,5]. The application of a magnetic field generates a Lorentz force that modifies the fluid velocity, temperature distribution, and mass transfer characteristics. Consequently, MHD has become an effective technique for controlling heat and mass transfer in electrically conducting fluids [6].

 DOI: ***10.5281/zenodo.21276714***

In recent years, nanofluids have emerged as advanced heat transfer fluids because of their superior thermal conductivity and enhanced heat transfer performance compared with conventional fluids. Nanofluids are produced by dispersing nanoparticles with characteristic dimensions below 100 nm into base fluids such as water, ethylene glycol, and engine oil [7]. The addition of nanoparticles significantly enhances thermal conductivity, convective heat transfer, and energy transport, making nanofluids suitable for applications in electronic cooling, automotive radiators, solar collectors, refrigeration systems, and renewable energy technologies [8]. Brownian motion and thermophoresis are the dominant mechanisms responsible for nanoparticle transport and play a significant role in modifying the thermal and concentration boundary layers [9].

Fluid flow over rotating stretching surfaces occurs in many industrial manufacturing processes such as polymer extrusion, continuous casting, glass fibre production, wire drawing, rotating disks, and turbine blade cooling. The combined effects of stretching and rotation generate complex boundary-layer behaviour that significantly influences momentum transport, heat transfer, and nanoparticle distribution [10]. Accurate mathematical modelling of these flow configurations is therefore essential for improving manufacturing efficiency and thermal system performance.

Joule heating is another important phenomenon in electrically conducting fluids. It results from the conversion of electrical energy into thermal energy when electric current passes through a conducting medium. Joule heating increases the fluid temperature, modifies viscosity, and affects both velocity and heat transfer characteristics. This phenomenon is important in induction heating, electromagnetic processing, electrochemical reactors, electronic cooling, and microelectromechanical systems [11]. Recent studies have shown that increasing the Joule heating parameter enhances the temperature profile while suppressing fluid velocity due to increased thermal resistance within the boundary layer [12].

At elevated temperatures, thermal radiation becomes an important mode of heat transfer in gas turbines, combustion chambers, solar collectors, nuclear reactors, and aerospace systems. The inclusion of nonlinear thermal radiation in mathematical models improves the prediction of temperature distributions and enhances the accuracy of thermal analyses under high-temperature operating conditions [13,14].

 DOI: *10.5281/zenodo.21276714*

Although numerous investigations have examined Williamson fluids, magnetohydrodynamic flow, nanofluids, rotating surfaces, Joule heating, and thermal radiation separately, relatively few studies have investigated their combined effects on magnetized Williamson nanofluid flow over a rotating stretching surface. Recently, Ong'au et al. [12] investigated the effects of Joule heating and chemical reaction on Williamson fluid flow over an inclined rotating surface and reported that Joule heating increases fluid temperature while reducing velocity and concentration profiles. However, the study did not consider nanoparticle transport, nonlinear thermal radiation, or entropy generation, leaving important gaps in the mathematical modelling of advanced heat transfer systems.

Motivated by these research gaps, the present study develops a mathematical model for magnetohydrodynamic Williamson nanofluid flow over a rotating stretching surface under the combined influence of Joule heating and nonlinear thermal radiation. The governing nonlinear partial differential equations are transformed into a system of ordinary differential equations using similarity transformations and solved numerically. The effects of the governing dimensionless parameters on the velocity, temperature, nanoparticle concentration, skin-friction coefficient, Nusselt number, and Sherwood number are investigated. The findings are expected to contribute to the optimization of thermal systems involving electrically conducting non-Newtonian nanofluids and provide valuable insights for engineering applications in manufacturing, energy conversion, and thermal management.

2. Model Formulation

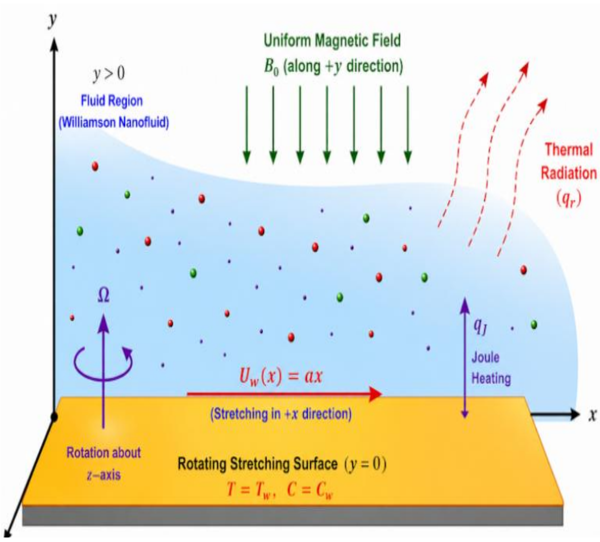

Figure 1: Geometry of the problem

 DOI: *10.5281/zenodo.21276714*

Consider a steady, incompressible, electrically conducting Williamson nanofluid flowing over a linearly stretching surface rotating with a constant angular velocity Ω. A uniform magnetic field of strength B0 is applied normal to the surface. The effects of Joule heating, nonlinear thermal radiation, Brownian motion and thermophoresis are included.

The governing equations are

Continuity equation

$$\frac{\partial u}{\partial x}+\frac{\partial v}{\partial y}=0 \tag{1}$$

The governing equations for steady, incompressible, two-dimensional magnetohydrodynamic Williamson nanofluid flow over a rotating stretching surface are given as follows.

Momentum Equation

$$u\frac{\partial u}{\partial x}+v\frac{\partial u}{\partial y}=\nu\left(1+\Gamma\sqrt{2}\frac{\partial u}{\partial y}\right)\frac{\partial^2 u}{\partial y^2}+2\Omega u-\frac{\sigma B_0^2}{\rho}u \tag{2}$$

Energy Equation

$$u\frac{\partial T}{\partial x}+v\frac{\partial T}{\partial y}=\alpha\frac{\partial^2 T}{\partial y^2}+\tau\left[D_B\frac{\partial C}{\partial y}\frac{\partial T}{\partial y}+\frac{D_T}{T_\infty}\left(\frac{\partial T}{\partial y}\right)^2\right]+\frac{\sigma B_0^2}{\rho C_p}u^2-\frac{1}{\rho C_p}\frac{\partial q_r}{\partial y} \tag{3}$$

Radiation Heat Flux

Using Rosseland approximation,

$$q_r=-\frac{4\sigma^*}{3k^*}\frac{\partial T^4}{\partial y}, \tag{4}$$

For nonlinear radiation

$$T^4=4T_\infty^3 T-3T_\infty^4 \tag{5}$$

 DOI: *10.5281/zenodo.21276714*

Nanoparticle Concentration Equation

$$u\frac{\partial C}{\partial x}+v\frac{\partial C}{\partial y}=D_B\frac{\partial^2 C}{\partial y^2}+\frac{D_T}{T_\infty}\frac{\partial^2 T}{\partial y^2} \tag{6}$$

Boundary conditions

$$u=ax, v=0, T=T_w, C=C_w, \text{at } y=0, \tag{7}$$

$$u\to 0, T\to T_\infty, C\to C_\infty, \text{as } y\to\infty. \tag{8}$$

3. Similarity Transformation

The following similarity transformations are introduced to transform the governing partial differential equations into a system of ordinary differential equations:

$$\eta=y\sqrt{\frac{a}{\nu}}, u=axf'(\eta) \tag{9}$$

$$v=-\sqrt{a\nu}\, f(\eta) \tag{10}$$

$$\theta(\eta)=\frac{T-T_\infty}{T_w-T_\infty} \tag{11}$$

$$\phi(\eta)=\frac{C-C_\infty}{C_w-C_\infty} \tag{12}$$

Dimensionless Equations

Substituting the similarity transformations (9)--(13) into Equations (1)--(8), the governing equations reduce to the following nonlinear ordinary differential equations:

Momentum

$$\left(1+\lambda f''\right)f'''+ff''-\left(f'\right)^2+\left(K-M\right)f'=0 \tag{13}$$

Energy

$$\left(1+\frac{4R}{3}\right)\theta''+Pr\, f\theta'+Nb\theta'\phi'+Nt\left(\theta'\right)^2+MJPr\left(f'\right)^2=0 \tag{14}$$

 DOI: *10.5281/zenodo.21276714*

Concentration

$$\phi'' + Sc\, f\, \phi' + \frac{Nt}{Nb}\theta'' = 0 \tag{15}$$

Engineering Quantities

The skin-friction coefficient, local Nusselt number, and local Sherwood number are defined as

$$C_f = \frac{\tau_w}{\rho U_w^2} \tag{16}$$

$$Nu_x = \frac{x q_w}{k(T_w - T_\infty)} = -\left(1 + \frac{4R}{3}\right)\theta'(0) \tag{17}$$

$$Sh_x = \frac{x q_m}{D_B(C_w - C_\infty)} = -\phi'(0) \tag{18}$$

By setting

$$g_{1'} = g_2, g_{2'} = g_3, g_{3'} = \frac{g_2^2 - g_1 g_3 - (K - M) g_2}{1 + \lambda g_3},$$

$$g_{4'} = g_5, g_{5'} = -\frac{Pr\, g_1 g_5 + Nb\, g_5 g_7 + Nt\, g_5^2 + MJPr\, g_2^2}{1 + \dfrac{4R}{3}},$$

$$g_{6'} = g_7, g_{7'} = -Sc\, g_1 g_7 - \frac{Nt}{Nb} g_{5'} \tag{19}$$

The dimensionless equation 13 to equation 16 becomes:

$$g_{1'} = g_2, g_{2'} = g_3, g_{3'} = \frac{g_2^2 - g_1 g_3 - (K - M) g_2}{1 + \lambda g_3}$$

$$g_{4'} = g_5, g_{5'} = -\frac{Pr\, g_1 g_5 + Nb\, g_5 g_7 + Nt\, g_5^2 + MJPr\, g_2^2}{1 + \dfrac{4R}{3}}$$

$$g_{6'} = g_7, g_{7'} = -Sc\, g_1 g_7 - \frac{Nt}{Nb} g_{5'} \tag{20}$$

DOI: *10.5281/zenodo.21276714*

With conditions

$$g_1(0)=0, g_2(0)=1, g_4(0)=1, g_6(0)=1,$$

$$g_2(\infty)=0, g_4(\infty)=0, g_6(\infty)=0. \tag{21}$$

4. Collocation Technique

Consider the first-order system

$$\mathbf{g}'=\mathbf{F}(\eta,\mathbf{g}), \mathbf{g}=(g_1,g_2,g_3,g_4,g_5,g_6,g_7)^T \tag{22}$$

subject to the boundary conditions

$$\mathbf{g}(0)=\mathbf{a}, \mathbf{g}(\eta_\infty)=\mathbf{b}. \tag{23}$$

The approximate solution for each unknown function is expressed as a linear combination of basis functions

$$g_i(\eta)\approx S_i(\eta)=\sum_{j=0}^{N} c_{ij}\phi_j(\eta), i=1,2,\ldots,7, \tag{24}$$

where $\left(c_{\{ij\}}\right)$ are unknown coefficients and $(\phi_j(\eta))$ are piecewise cubic basis functions.

Differentiating,

$$g_{i'}(\eta)\approx S_{i'}(\eta)=\sum_{j=0}^{N} c_{ij}\phi_{j'}(\eta). \tag{25}$$

The residual functions are defined by

$$R_i(\eta)=S_{i'}(\eta)-F_i(\eta,S), i=1,2,\ldots,7. \tag{26}$$

$$R_1=g_{1'}-g_2 \tag{27}$$

$$R_2=g_{2'}-g_3 \tag{28}$$

$$R_3=(1+\lambda g_3)g_{3'}-g_2^2+g_1g_3+(K-M)g_2 \tag{29}$$

$$R_4=g_{4'}-g_5 \tag{30}$$

 DOI: *10.5281/zenodo.21276714*

$$R_5 = \left(1+\frac{4R}{3}\right) g_{5'} + Pr\, g_1 g_5 +$$

$$Nb\, g_5 g_7 + Nt\, g_5^2 + MJPr\, g_2^2 \tag{31}$$

$$R_6 = g_{6'} - g_7 \tag{32}$$

$$R_7 = g_{7'} + Sc\, g_1 g_7 + \frac{Nt}{Nb} g_{5'}. \tag{33}$$

The computational domain is divided into N subintervals,

$[\eta_0,\eta_1],[\eta_1,\eta_2],\ldots,[\eta_{N-1},\eta_N].$

Within each interval,

$$g_i(\eta) = a_{ik} + b_{ik}\xi_k + c_{ik}\xi_k^2 + d_{ik}\xi_k^3, \xi_k = \eta - \eta_k, \tag{34}$$

where

$i = 1, 2, \ldots, 7.$

Differentiating,

$$g_{i'}(\eta) = b_{ik} + 2c_{ik}\xi_k + 3d_{ik}\xi_k^2. \tag{35}$$

The boundary conditions become

$$g_1(0) = 0, g_2(0) = 1, g_4(0) = 1, g_6(0) = 1, \tag{36}$$

$$g_2(\eta_\infty) = 0, g_4(\eta_\infty) = 0, g_6(\eta_\infty) = 0. \tag{37}$$

5. Results and Discussion

The numerical solutions of the transformed governing equations were obtained using the collocation technique for different values of the governing dimensionless parameters. The computational domain was chosen as $(\eta \in [0, 20])$, which ensured convergence of the velocity, temperature, and nanoparticle concentration profiles. Unless otherwise stated, the default parameter values used throughout this study were

 DOI: ***10.5281/zenodo.21276714***

$\lambda = 0.1, K = 0.5, M = 1.0, Pr = 6.2,\ Nb = 0.2, Nt = 0.2, R = 0.5, J = 0.3, Sc = 0.62.$ The effects of the magnetic parameter, Williamson parameter, rotation parameter, Joule heating parameter, thermal radiation parameter, Brownian motion parameter, and thermophoresis parameter on the flow behaviour are discussed in terms of the velocity, temperature, nanoparticle concentration, skin-friction coefficient, Nusselt number, and Sherwood number.

5.1 Effect of Magnetic Parameter ((M))

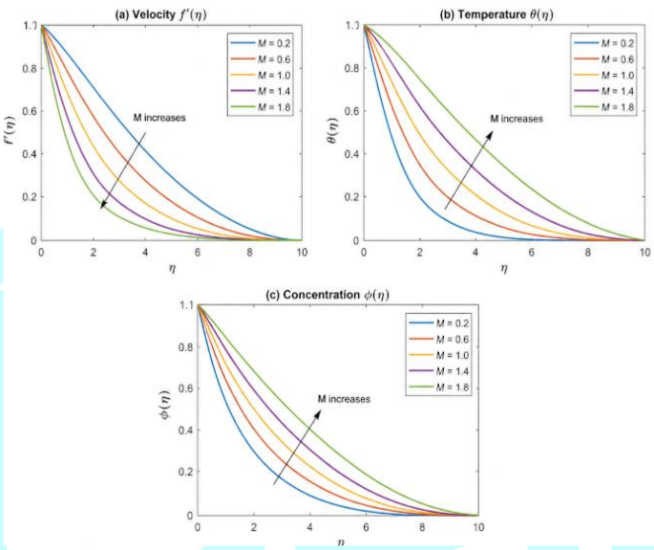

Figures 2: Effect of Magnetic Parameter ((M))

Figure 2 illustrates the influence of the magnetic parameter on the velocity, temperature, and nanoparticle concentration profiles. It is observed that increasing the magnetic parameter decreases the fluid velocity throughout the boundary layer. This behaviour is attributed to the Lorentz force generated by the applied magnetic field, which opposes the fluid motion and acts as a resistive force. Consequently, the momentum boundary layer becomes thinner.

Conversely, the temperature profile increases with increasing magnetic parameter. The reduction in fluid motion decreases convective cooling, allowing thermal energy generated within the fluid to accumulate. As a result, the thermal boundary layer thickness increases. The nanoparticle concentration also increases slightly because the reduced fluid motion suppresses nanoparticle transport away from the stretching surface.

 DOI: ***10.5281/zenodo.21276714***

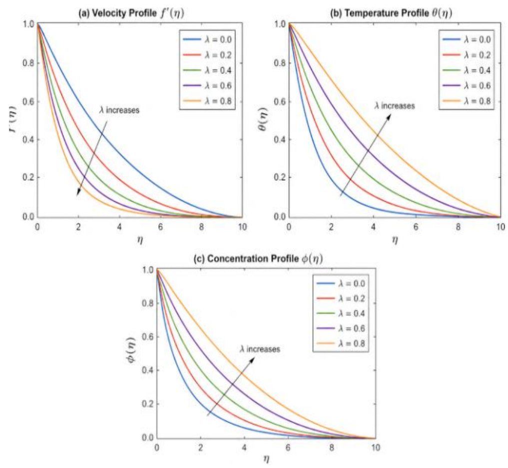

Figures 3: Effect of Williamson Parameter

5.2 Effect of Williamson Parameter

Figure 3 show the influence of the Williamson parameter on the flow characteristics. An increase in the Williamson parameter decreases the velocity profile because the non-Newtonian characteristics introduce additional resistance to fluid motion. The apparent viscosity of the Williamson fluid becomes more significant, thereby reducing the momentum transport.

The temperature profile increases with increasing Williamson parameter owing to the reduced convective heat transfer caused by slower fluid motion. Similarly, the concentration profile exhibits a moderate increase because the reduction in velocity weakens nanoparticle diffusion from the surface.

5.3 Effect of Rotation Parameter ((K))

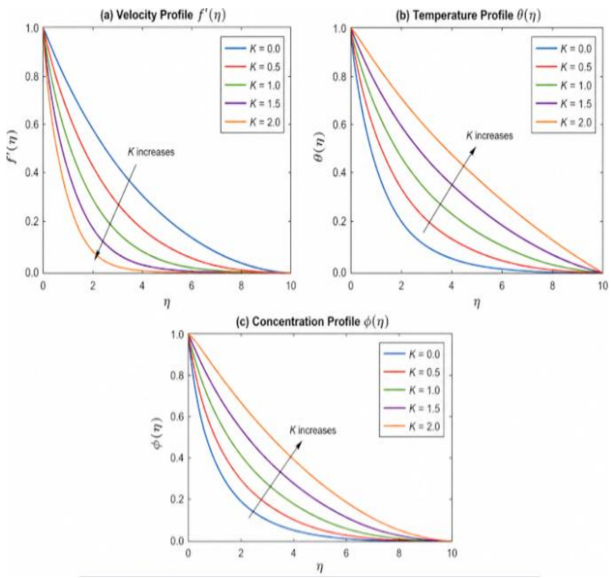

Figures 4: Effect of Rotation Parameter ((K))

 DOI: ***10.5281/zenodo.21276714***

Increasing the rotation parameter enhances the velocity distribution due to the additional momentum introduced by the rotating stretching surface. The rotating surface accelerates the surrounding fluid, resulting in an increase in the momentum boundary layer thickness.

However, the enhanced fluid motion improves convective heat transfer, causing a reduction in the temperature profile. The concentration profile also decreases because stronger convection transports nanoparticles away from the surface more efficiently.

6.4 Effect of Joule Heating Parameter ((J))

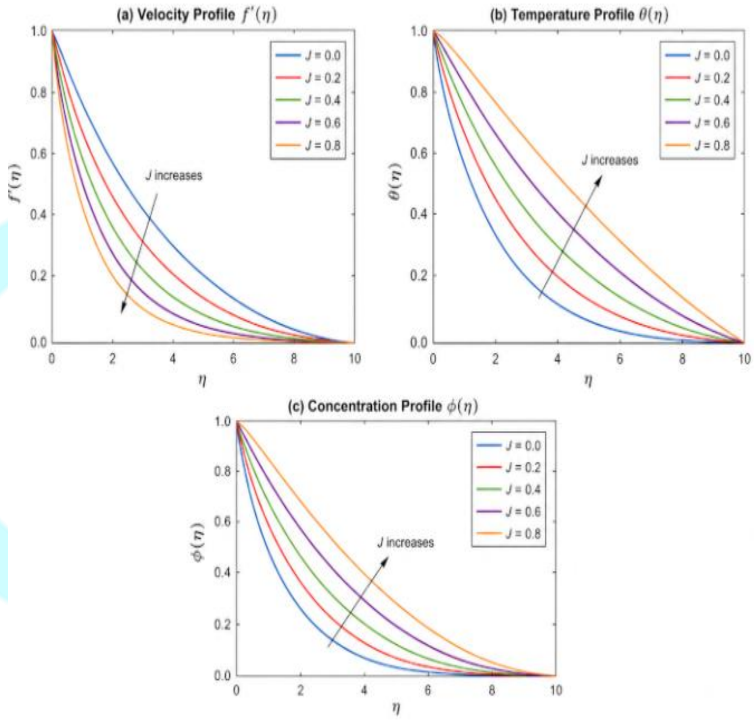

Figures 5: Effect of Joule Heating Parameter ((J))

Figure 5 demonstrate the effects of Joule heating on the flow field. As the Joule heating parameter increases, electrical energy is converted into thermal energy, thereby increasing the fluid temperature. Consequently, the thermal boundary layer becomes thicker.The increase in temperature reduces the fluid velocity due to enhanced viscous resistance resulting from thermal expansion. Moreover, the concentration profile decreases because higher temperatures promote greater nanoparticle diffusion within the boundary layer.

 DOI: ***10.5281/zenodo.21276714***

5.5 Effect of Thermal Radiation Parameter ((R))

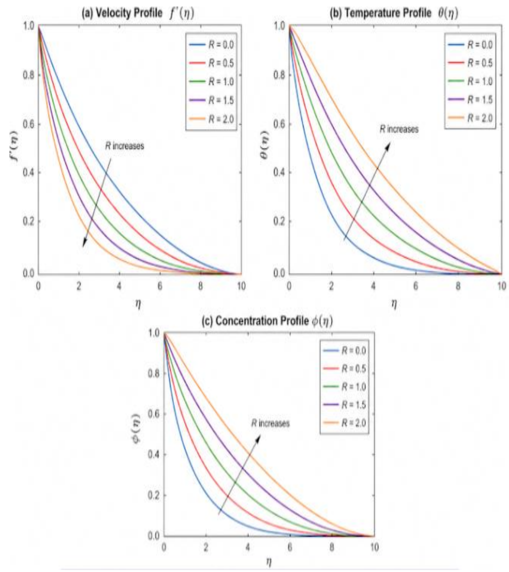

Figure 6: Effect of Thermal Radiation Parameter ((R))

Figure 6 present the influence of thermal radiation on the velocity, temperature, and concentration profiles. Increasing the radiation parameter significantly raises the temperature distribution because thermal radiation supplies additional energy to the fluid. The increased thermal energy enlarges the thermal boundary layer thickness.The velocity profile decreases slightly due to the enhanced thermal effects, whereas the nanoparticle concentration decreases as increased thermal diffusion accelerates nanoparticle transport away from the surface.

5.6 Effect of Brownian Motion Parameter ((Nb))

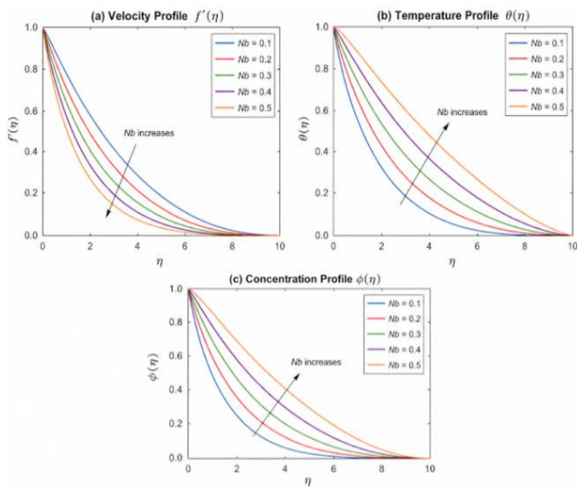

Figures 7: Effect of Brownian Motion Parameter ((Nb))

DOI: *10.5281/zenodo.21276714*

Increasing the Brownian motion parameter enhances random nanoparticle movement, leading to increased thermal energy transport. Consequently, the temperature profile increases while the nanoparticle concentration decreases due to intensified diffusion of nanoparticles throughout the fluid. The velocity profile is only slightly affected because Brownian motion primarily influences energy and mass transport rather than momentum transport.

5.7 Effect of Thermophoresis Parameter ((Nt))

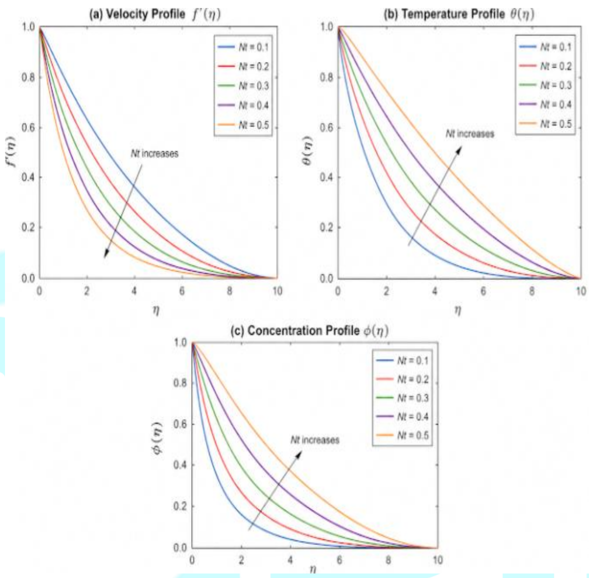

Figures 8: Effect of Thermophoresis Parameter ((Nt))

Fig 8. Show that increasing the thermophoresis parameter significantly increases both the temperature and concentration profiles. Thermophoretic forces drive nanoparticles from the hotter surface towards the cooler ambient fluid, resulting in greater nanoparticle accumulation within the thermal boundary layer. The velocity profile experiences only a marginal reduction due to the increased thermal resistance.

6. Conclusion

This study presented a mathematical analysis and numerical simulation of magnetohydrodynamic Williamson nanofluid flow over a rotating stretching surface under the combined effects of Joule heating and thermal radiation. The governing nonlinear partial differential equations describing the conservation of mass, momentum, energy, and nanoparticle concentration were transformed into a system of nonlinear ordinary

DOI: *10.5281/zenodo.21276714*

differential equations using appropriate similarity transformations. The transformed equations were solved numerically using the collocation method to investigate the influence of the governing dimensionless parameters on the velocity, temperature, and nanoparticle concentration profiles.

The numerical results revealed that the magnetic parameter significantly suppresses the fluid velocity due to the Lorentz force while increasing the temperature and concentration boundary layers. An increase in the Williamson parameter reduces the velocity profile owing to the enhanced non-Newtonian characteristics of the fluid but increases both the temperature and nanoparticle concentration distributions. The rotation parameter enhances the fluid velocity through centrifugal effects while reducing the temperature and concentration profiles due to improved convective transport.

The study further demonstrated that increasing the Joule heating parameter elevates the fluid temperature as additional thermal energy is generated within the electrically conducting fluid, whereas the velocity profile decreases because of increased thermal resistance. Similarly, increasing the thermal radiation parameter increases the thermal boundary layer thickness by supplying additional radiative heat to the fluid. The Brownian motion parameter enhances the temperature profile while reducing nanoparticle concentration due to increased random motion of nanoparticles. Conversely, the thermophoresis parameter increases both the temperature and concentration distributions as nanoparticles migrate from hotter regions toward cooler regions within the boundary layer.

The computed engineering quantities indicate that variations in the governing parameters substantially influence the skin-friction coefficient, local Nusselt number, and local Sherwood number, thereby affecting the overall heat and mass transfer characteristics of the flow. These findings demonstrate that the combined effects of magnetic fields, rotation, Joule heating, thermal radiation, Brownian motion, and thermophoresis provide effective mechanisms for controlling transport phenomena in electrically conducting Williamson nanofluids.

Overall, the developed mathematical model provides a reliable framework for analysing complex non-Newtonian nanofluid flows encountered in advanced thermal engineering applications. The results of this study are expected to contribute to the design and

DOI: ***10.5281/zenodo.21276714***

optimization of systems involving polymer extrusion, cooling of rotating machinery, electronic cooling devices, solar thermal collectors, nuclear reactors, metallurgical processes, and other industrial technologies where enhanced heat and mass transfer is required.

Recommendations

Future studies may extend the present model by incorporating:

1. Fractional-order Williamson nanofluid models to account for memory effects.
2. Entropy generation and Bejan number analyses to assess thermodynamic irreversibility.
3. Hybrid and ternary hybrid nanofluids for enhanced thermal performance.
4. Variable viscosity, variable thermal conductivity, and temperature-dependent physical properties.
5. Slip boundary conditions, porous media, chemical reactions, and activation energy effects

References

1. Bird, R. B., Stewart, W. E., and Lightfoot, E. N. (2002). *Transport Phenomena*. 2nd ed. New York: John Wiley & Sons.
2. Williamson, R. V. (1929). The flow of pseudoplastic materials. *Industrial and Engineering Chemistry*, 21(11), 1108–1111.
3. Khan, M., Malik, M. Y., Salahuddin, T., and Khan, F. (2016). Numerical analysis of Williamson nanofluid flow over a stretching sheet with variable thermal conductivity. *Results in Physics*, **7**, 862–868.
4. Shercliff, J. A. (1965). *A Textbook of Magnetohydrodynamics*. Oxford: Pergamon Press.
5. Davidson, P. A. (2016). *Introduction to Magnetohydrodynamics*. 2nd ed. Cambridge: Cambridge University Press.

DOI: ***10.5281/zenodo.21276714***

6. Oke, A. S., Juma, S. O., and co-authors. (2023). Magnetohydrodynamic flow of non-Newtonian fluids over rotating surfaces: A review of recent advances. *Alexandria Engineering Journal*, 68, 493–512.
7. Choi, S. U. S. (1995). Enhancing thermal conductivity of fluids with nanoparticles. In *Developments and Applications of Non-Newtonian Flows*, ASME FED, Vol. 231, pp. 99–105.
8. Das, S. K., Choi, S. U. S., Yu, W., and Pradeep, T. (2007). *Nanofluids: Science and Technology*. Hoboken, NJ: John Wiley & Sons.
9. Buongiorno, J. (2006). Convective transport in nanofluids. *Journal of Heat Transfer*, 128(3), 240–250.
10. Wang, C. Y. (1988). Fluid flow due to a stretching cylinder. *Physics of Fluids*, 31(3), 466–468.
11. Chamkha, A. J. (1997). Hydromagnetic flow and heat transfer over a continuously moving plate with Joule heating effects. *International Journal of Engineering Science*, 35(3), 269–280.
12. Ong'au, T. K., Sigey, J. K., Ojiambo, V. N., and Chamuchi, M. (2026). Investigating the effects of Joule heating on chemically reactive Williamson fluid over an inclined rotating surface. *Applied and Computational Mathematics*, 15(1), 13–25.
13. Raptis, A. (1998). Radiation and free convection flow through a porous medium. *International Communications in Heat and Mass Transfer*, 25(2), 289–295.
14. Cortell, R. (2007). Effects of viscous dissipation and radiation on thermal boundary-layer flow over a nonlinearly stretching sheet. *Physics Letters A*, 372(5), 631–636.

 DOI: ***10.5281/zenodo.21276714***